

Hysteretic Memory Effects in Disordered Magnets

Helmut G. Katzgraber¹ and György T. Zimányi²

¹Theoretische Physik, ETH Hönggerberg, CH-8093 Zurich, Switzerland

²Physics Department, University of California, Davis, CA 95616, USA

(Dated: February 8, 2020)

We study the return point as well as the complementary point memory effects numerically with paradigmatic models for random magnets and show that already simple systems with Ising spin symmetry can reproduce the experimental results of Pierce et al. where both memory effects become more pronounced for increasing disorder and return point memory is always better than complementary point memory.

PACS numbers: 75.50.Lk, 75.40.Mg, 05.50.+q

Hysteresis is ubiquitous in nature: it occurs in interacting systems as a collective phenomenon, in most disordered systems, across first order transitions, in magnetic systems, and in depinning phenomena, among others. It is also crucial for industrial applications: most notably hysteresis lies at the very foundation of the magnetic recording industry. Hysteretic systems are employed as recording media because they retain their state for a long period after a write operation: they exhibit memory. Many aspects of this memory effect have been studied, e.g., the long-time decay of information through the superparamagnetic decay [1] or how to optimize the signal-to-noise ratio by magnetic modeling, among others.

Because of the central importance of memory in recording media, other types of memory have been studied as well. Pierce et al. [2] have investigated Co/Pt multilayer

in s by repeated cycling over the hysteresis loop. The macroscopic magnetization returns to the same value cycle after cycle, signature of a further type of memory. It is a profound question whether this memory comes about by the system returning to the same microscopic configuration: an effect dubbed "Return Point Memory" (RPM), or this memory is exhibited only on the macroscopic level. Using X-ray microscopy techniques, Pierce et al. have found the presence of RPM for strong disorder, but no RPM for weak disorder. Furthermore, Pierce et al. have studied a second type of memory: whether the system develops the reverse of the original configuration when the hysteresis sweep reaches the opposite magnetic field, called "Complementary Point Memory" (CPM). They have found that the disorder influences CPM the same way as RPM. In addition, they report that CPM appears to be smaller than RPM. However, the RPM-CPM difference does not exceed 10% and it is not clear whether the difference could have been caused by instrumental bias.

The experimental work of Pierce et al. has spawned two theoretical studies to date: Deutsch and Mai have performed microscopic simulations using the Landau Lifshitz Gilbert (LLG) equations [3] and reproduce the above memory effects. However, only few disorder realizations have been considered, leading to large error bars.

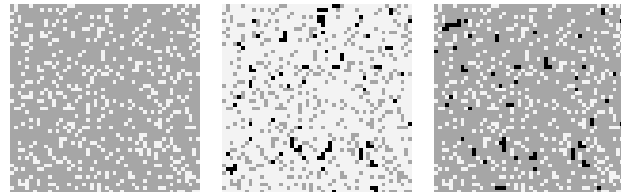


FIG. 1: Configurations for $j_1 = j_2 = 12$ for the 2D Edwards-Anderson Ising spin glass at zero temperature. Light pixels correspond to down spins, dark pixels correspond to up spins. Left: initial configuration at $H = 12$. Center: configuration after a half cycle at $H = -H$ (CPM). Right: configuration at $H = H$ after one cycle around the hysteresis loop (RPM). The black pixels represent differences between the initial and final configurations.

Furthermore, the difference between RPM and CPM is not much bigger than the error bars of the simulation. Finally, they suggest that the rotation of spins is primarily responsible for the RPM-CPM difference, i.e., scalar spins cannot cause the effect (in the absence of random fields). But since their Hamiltonian contains numerous terms with seven parameters, further clarification may be useful to determine which of these terms is the primary cause of the memory effect. Jagla has also used the LLG approach, but for constrained soft scalar spins subject to random fields [4]. He reports seeing the memory effect and the RPM-CPM difference as well. However, no quantitative measure of the memory has been given and the simulations have been performed only at $T = 0$.

Therefore, the following challenges still remain to be understood: (i) what is the primary cause of the memory effect, or equivalently, what is the minimal model, that exhibits the memory effect, (ii) does the memory effect persist at finite temperatures, since thermal fluctuations have the potential to destroy microscopic correlations, (iii) what is the disorder dependence of the memory effects and (iv) does the RPM-CPM difference convincingly exceed the error bars? To address these challenges, we have studied RPM and CPM in minimal, paradigmatic disordered spin models: spin glasses and random-field models. Equilibrium and close to equi-

librium dynamical properties of spin glasses have been studied extensively over the years [5, 6, 7]. However, far from equilibrium properties, such as their hysteresis, are less understood. Recent studies have characterized the hysteresis loop of the Edwards-Anderson Ising spin glass (EA SG) [8], the Random Field Ising Model (RFIM) [9], and the Sherrington-Kirkpatrick model [10]. However, microscopic correlations and memory effects have not been considered to date. In this paper we report studies of memory effects in disordered spin models with and without frustration to address the above challenges.

We first study the Edwards-Anderson Ising spin glass [5] with the Hamiltonian

$$H_{\text{EA SG}} = \sum_{\langle i,j \rangle} J_{ij} S_i S_j - H \sum_i S_i \quad (1)$$

in which Ising spins $S_i = \pm 1$ lie on the sites of a square lattice in two dimensions (2D) of size $N = L^2$ with periodic boundary conditions. The measured quantities converge rapidly and show essentially no size-dependence past $L = 20$. The interactions J_{ij} are Gaussian distributed with zero mean and standard deviation J . The simulations are performed by first saturating the system by applying a large external field H and then reducing H in small steps to reverse the magnetization. At zero temperature we use Glauber dynamics [8] where randomly chosen unstable spins (pointing against their local field $h_i = \sum_{j \neq i} J_{ij} S_j + H$) are flipped until all spins are stable for each field step. At finite temperatures we perform a Monte Carlo simulation and equilibrate until the average magnetization is independent of time for each field step. All results are averaged over 500 disorder realizations.

Pierce et al. have captured the return and complementary point memory of their experimental system in terms of overlaps of the spin configurations in Fourier space before and after hysteretic protocols. Accordingly, we capture CPM and RPM with $q(H)$, the overlap of the spin configuration at a field H with the configuration at a field with the same magnitude $|H|$ after $n = 1/2$ and 1 cycle around the hysteresis loop, respectively:

$$q(H) = \frac{(-1)^{2n} \sum_{i=1}^N S_i(H) S_i^{(n)}(H)}{N} : \quad (2)$$

The uniqueness of CPM/RPM is tested by $q^0(H)$, the overlap between a configuration at H with all configurations after 1/2 and 1 cycle around the hysteresis loop:

$$q^0(H) = \frac{(-1)^{2n} \sum_{i=1}^N S_i(H) S_i^{(n)}(H)}{N} : \quad (3)$$

To develop a physical picture, Fig. 1 depicts configuration snapshots of the 2D EA SG illustrating CPM and RPM. The EA SG displays a large degree of CPM/RPM configurational memory. However, even at $T = 0$ this memory is not perfect for this frustrated model.

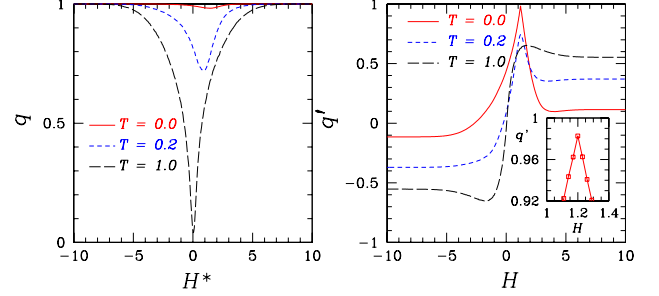


FIG. 2: (Color Online) Overlaps for the 2D EA SG. Left: Overlap q [Eq. (2)] for different values of H^* at different temperatures T . Right: Overlap q^0 [Eq. (3)] as a function of the applied field H for $H = 1.2$. The memory becomes more pronounced for $T \neq 0$, but is not perfect even at $T = 0$ (inset). Data for $j = 1$.

On the quantitative level, Fig. 2, left panel shows $q(H^*)$ as a function of H^* for various temperatures. The RPM and CPM curves are indistinguishably close. The system exhibits nearly complete CPM/RPM throughout the entire field range at $T = 0$. The strong CPM can be attributed to the spin-reversal symmetry of the system: upon reversing all spins S_i and the magnetic field H , the Hamiltonian transforms into itself. The observation of robust RPM and CPM answers the aforementioned challenge (i) by establishing the EA SG as a minimal model displaying memory effects such as in the experiments of Pierce et al. with no adjustable parameters.

Note that the memory is not perfect even at $T = 0$. This is probably due to the stochastic nature of the updating: during the field sweep spins are selected randomly for updating. Therefore, even at $T = 0$, the spin configurations do not evolve entirely along the same valleys of the energy landscape. This incompleteness of CPM and RPM could not be detected in simulations of long-range forces and continuous spins, where the large error bars mask this effect entirely. Also noteworthy is that CPM/RPM is smallest around the (temperature dependent) coercive field, as the number of equivalent spin configurations is the largest in that field region, thus the reversal process can evolve along many different paths.

We also address the temperature dependence of the overlap, as raised in point (ii). Figure 2 shows that CPM and RPM survive at finite T , even though it would be natural for the thermal fluctuations to wash out the microscopic memory and convert it to a macroscopic memory only. Our data show that CPM/RPM decrease with increasing temperature, as expected.

Figure 2, right panel shows $q^0(H)$ at $H = 1.2$ for various temperatures. The data show the uniqueness of CPM and RPM: the overlap peaks only at $H = H$. Thus, the memory is not the result of a gradual slow buildup, moreover there are large-scale spin rearrangements during the field sweep in frustrated systems, repre-

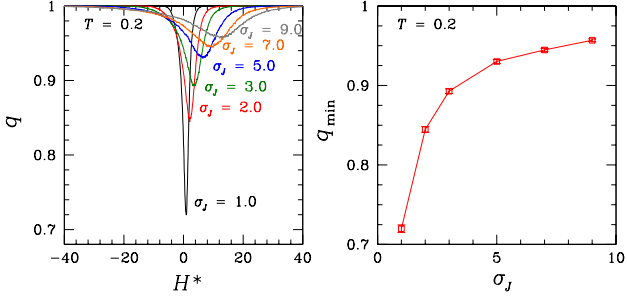


FIG. 3: (Color Online) Left panel: overlap $q(H^*)$ for RPM/CPM (2D EA SG) as a function of H^* for different disorder strengths σ_J . Right panel: minimum value (at coercivity) of $q(H^*)$ as a function of disorder for RPM/CPM. The memory increases with increasing disorder.

ating the initial spin configuration only in the vicinity of $H = H^*$.

As above, CPM and RPM are not perfect even at $T = 0$ (inset of Fig. 2) and decrease with increasing temperature. Furthermore, the nonzero plateaus are caused by the measuring field $H = 1.2$ being different from the coercive field, where the magnetization $M(H)$ is nonzero. $M(H)$ increases with increasing temperature as the coercive field moves away from $H = 1.2$ with increasing T . The plateau values, which give the overlap of a fully polarized state with the state with magnetization $M(H)$, grow with increasing T accordingly.

We discuss next the disorder dependence of both memory effects, an important aspect in the experimental results of Pierce et al., and address point (iii). Figure 3, left panel shows $q(H^*)$ as a function of H^* , indexed by the disorder σ_J at $T = 0.2$. The right panel of Fig. 3 shows $q(H^*)$ at coercivity as a function of σ_J . Visibly, RPM/CPM increase dramatically with increasing disorder, in good agreement with the experiments of Pierce et al. The physical reason for this correlation is that for weak disorder, the energy landscape includes many comparable shallow valleys without a single optimal path. Therefore, during subsequent field sweeps, the system evolves along different paths, thus reducing the memory. In contrast, for stronger disorder, the energy landscape develops a few preferable valleys and the system evolves along these optimal valleys. The dips in $q(H^*)$ become broader with increasing disorder because the entire hysteresis loop broadens. Finally, in relation to point (iv) it is noted that in the EA SG the differences between RPM and CPM are measurably small.

Next, we study the same memory effects and challenges in the 2D random-field Ising model:

$$H_{\text{RFIM}} = \sum_{\langle i,j \rangle} J S_i S_j + \sum_i h_i S_i : \quad (4)$$

Here $J = 1$ is a ferromagnetic coupling and the random fields h_i are chosen from a Gaussian distribution

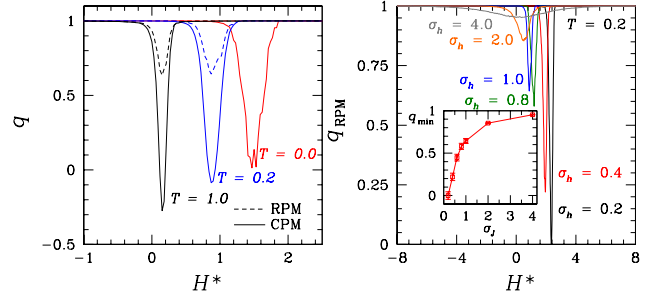


FIG. 4: (Color Online) Left panel: Overlap q for RPM (dashed lines) and CPM (solid lines) for different temperatures for the RFIM. RPM is perfect at $T = 0$. For all temperatures RPM is better than CPM. In particular, for all temperatures CPM is close to zero at coercivity suggesting that CPM is rather poor in this model. Right panel: Field dependence of $q(H^*)$ for RPM for different disorder strengths σ_h ($T = 0.20$). RPM improves with increasing disorder at finite temperatures. The inset shows the disorder dependence of $q(H^*)$ at coercivity (RPM).

with zero mean and standard deviation σ_h . The main differences between the RFIM and the EA SG are that the RFIM does not have frustration and does not have spin-reversal symmetry.

Figure 4, left panel shows both $q(H^*)$ for RPM (dashed lines) and CPM (solid lines) as a function of H^* for various temperatures. Regarding (i), this model also exhibits memory, both RPM and CPM, thus establishing another simple model exhibiting the experimentally measured memory effects. Furthermore, (ii) the effects also are not washed out by thermal fluctuations at once, but are gradually weakened with increasing T .

Regarding (iv), the RFIM deviates from the EA SG results and correlates with the experiments: in the RFIM, RPM and CPM are different. RPM is bigger than CPM for all temperatures. This effect is due to the fact that the RFIM does not have spin-reversal symmetry and therefore the spin configurations on the ascending branch do not correlate closely with the configurations on the descending branch. For intermediate-to-large values of the disorder, CPM is negligible and, in the proximity of the coercive field, the CPM correlation is even negative. In contrast, RPM is large in the RFIM. In particular, at $T = 0$ RPM is perfect due to the "no-crossing property" of the RFIM [11]. This is in contrast to the frustrated EA SG where RPM is never perfect. Figure 4, right panel shows (iii) $q(H^*)$ for RPM for different disorder strengths σ_h at $T = 0.2$. The memory in the RFIM also increases with increasing disorder. The inset shows the overlap $q(H^*)$ at coercivity for RPM, which clearly increases with increasing disorder. As for the EA SG, memory increases due to the valleys in the energy landscape becoming more pronounced with increasing disorder.

In the RFIM, CPM is always close to zero whereas RPM increases with increasing disorder and is perfect at

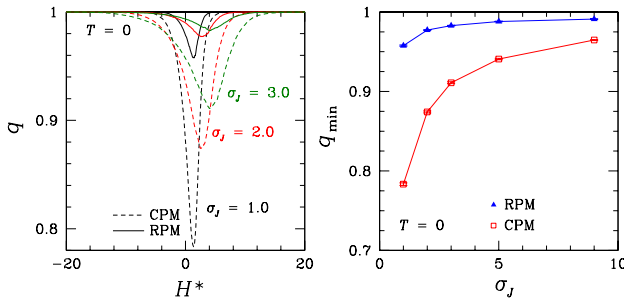


FIG. 5: (Color Online) Left panel: Field dependence of $q(H^*)$ for RPM (solid lines) and CPM (dashed lines) for different disorder strengths σ_J ($T = 0$) for the SG + RF model [Eq. (5)]. Right panel: Disorder dependence of $q(H^*)$ of RPM and CPM at coercivity. Both memory effects increase with increasing disorder and RPM is always larger than CPM, in agreement with the experimental results of Pierce et al.

$T = 0$. Correspondingly, the RPM - CPM difference is large over much of the parameter space. These findings do not agree with the experimental results of Pierce et al. The EA SG lacks the RPM - CPM asymmetry completely, again in contradiction with the experiments, prompting the question of whether a combination of the EA SG and the RFIM might yield results comparable to the experiments: increasing memory with increasing disorder, as well as RPM being better than CPM. Thus we introduce random fields into the EA SG that act only on a small fraction (5%) of the spins in order to break the spin-reversal symmetry of the Hamiltonian [Eq. (1)]:

$$H_{SG+RF} = \sum_{\langle i,j \rangle} J_{ij} S_i S_j + \sum_i h_i S_i : \quad (5)$$

The random bonds J_{ij} are chosen from a Gaussian distribution with zero mean and standard deviation σ_J . The random fields are chosen from a Gaussian distribution with zero mean and standard deviation unity.

Figure 5 shows the results at $T = 0$ which also persist at finite T (not shown). The left panel of Fig. 5 shows $q(H^*)$ for both RPM and CPM as a function of H^* for different disorder strengths σ_J . The right panel of Fig. 5 shows the overlap q at coercivity: both memory effects increase with increasing disorder and RPM is larger than CPM, thus establishing that the SG + RF model closely tracks semiquantitatively all aspects of the Pierce et al. experiments.

In summary, we have simulated paradigmatic disordered spin models: the Edwards-Anderson spin glass, the random-field Ising model and a spin glass with diluted random fields, Eq. (5). We have found that: (i) All three models exhibit return point (RPM) as well as complementary point (CPM) memory. (ii) Both memory effects persist to finite temperatures. (iii) Both memory effects increase with increasing disorder. (iv) In the spin glass,

RPM and CPM are identical because of the spin-reversal symmetry. In the RFIM, RPM is always considerably better than CPM because of the lack of spin-reversal symmetry. Finally, a spin glass with diluted random fields breaking spin-reversal symmetry reproduces the experimental results of Pierce et al: the model exhibits RPM and CPM, both memory effects increase with increasing disorder, and RPM is better than CPM.

In relation to the experiments of Pierce et al, one recalls that the ins of Pierce et al have strong out-of-plane anisotropy, restricting the orientation of the spins to being perpendicular to the ins. Thus, describing those ins in terms of Ising spins might be an acceptable approximation. Furthermore, since the dipolar interactions in these perpendicular ins are antiferromagnetic, they introduce extensive frustration into the system, the key ingredient of spin glasses. Finally, spins frozen in by shape anisotropies of a locally deformed environment, or by unusually large crystal-field anisotropies, or by frozen-in reversed bubbles, as reported by Davies et al. in Co/Pt multilayer ins [12], can all possibly be the origin of random fields coupling to some sites. These considerations make it conceivable that all ingredients of the SG + RF model may be present in the experimental ins.

Our results could be viewed in the context of the approaches of Dentsch and Mai as well as Jagla, who have employed vector and continuous spin models with LLG dynamics, respectively. Their models both contain several terms and corresponding parameters. On balance, one may take the position that the SG + RF model, Eq. (5), reproduces qualitatively all aspects of the experiments within a minimal framework.

We acknowledge useful discussions with E. E. Fullerton, O. Hellwig, L. Sorensen, Kai Liu, R. T. Scalettar and J. M. Dentsch.

- [1] S. H. Charap, L. Pu-Ling, and H. Yanjin, IEEE Trans. Magn. 33, 978 (1997).
- [2] M. S. Pierce et al., Phys. Rev. Lett. 94, 017202 (2005).
- [3] J. M. Dentsch and T. Mai, Phys. Rev. E 72, 016115 (2005).
- [4] E. A. Jagla, (cond-mat/0412461) (2004).
- [5] K. Binder and A. P. Young, Rev. Mod. Phys. 58, 801 (1986).
- [6] A. P. Young, ed., Spin Glasses and Random Fields (World Scientific, Singapore, 1998).
- [7] N. Kawashima and H. Rieger (2003), (cond-mat/0312432).
- [8] H. G. Katzgraber et al., Phys. Rev. Lett. 89, 257202 (2002).
- [9] J. P. Sethna et al., Phys. Rev. Lett. 70, 3347 (1993).
- [10] F. Pazmandi, G. Zarand, and G. T. Zimanyi, Phys. Rev. Lett. 83, 1034 (1999).
- [11] A. A. Middleton, Phys. Rev. Lett. 68, 670 (1992).
- [12] J. E. Davies et al., Appl. Phys. Lett. 86, 2503 (2005).